NREL/TP-471-7294 • UC Category: 1303 • DE95000219

Flux Attenuation at NREL's High-Flux Solar Furnace

Carl E. Bingham
Kent L. Scholl
Allan A. Lewandowski
National Renewable Energy Laboratory

Prepared for the ASME/JSME/JSES International Solar Energy Conference, Maui, HI, March 19–24, 1995

National Renewable Energy Laboratory
1617 Cole Boulevard
Golden, Colorado 80401-3393

A national laboratory of the U.S. Department of Energy
managed by Midwest Research Institute
for the U.S. Department of Energy
under Contract No. DE-AC36-83CH10093

October 1994

NOTICE

Available to DOE and DOE contractors from:
Office of Scientific and Technical Information (OSTI)
P.O. Box 62
Oak Ridge, TN 37831
Prices available by calling (615) 576-8401

Available to the public from:
National Technical Information Service (NTIS)
U.S. Department of Commerce
5285 Port Royal Road
Springfield, VA 22161
(703) 487-4650

Printed on paper containing at least 50% wastepaper and 10% postconsumer waste

FLUX ATTENUATION AT NREL'S HIGH-FLUX SOLAR FURNACE

Carl E. Bingham, Kent L. Scholl, Allan A. Lewandowski
Thermal Systems Branch
National Renewable Energy Laboratory
Golden, Colorado

ABSTRACT

The High-Flux Solar Furnace (HFSF) at the National Renewable Energy Laboratory (NREL) has a faceted primary concentrator and a long focal-length-to-diameter ratio (due to its off-axis design). Each primary facet can be aimed individually to produce different flux distributions at the target plane. Two different types of attenuators are used depending on the flux distribution. A sliding-plate attenuator is used primarily when the facets are aimed at the same target point. The alternate attenuator resembles a venetian blind. Both attenuators are located between the concentrator and the focal point. The venetian-blind attenuator is primarily used to control the levels of sunlight falling on a target when the primary concentrators are not focused to a single point.

This paper will demonstrate the problem of using the sliding-plate attenuator with a faceted concentrator when the facets are not aimed at the same target point. We will show that although the alternate attenuator necessarily blocks a certain amount of incoming sunlight, even when fully open, it provides a more even attenuation of the flux for alternate aiming strategies.

INTRODUCTION

The High-Flux Solar Furnace

The High-Flux Solar Furnace at NREL uses an off-axis design, a faceted primary concentrator, and a long focal-length-to-diameter ratio of 1.85 (Bingham and Lewandowski, 1991). Each of the 25 primary facets can be aimed individually to produce different flux distributions at the target plane. With all primary facets aimed to the same point, the flux distribution of the primary concentrator is nearly Gaussian, with more than 95% of the energy falling within a 10-cm diameter. The furnace is also designed to accommodate non-imaging secondary concentrators, which can produce concentrations of up to 50,000 suns (Jenkins et al., 1994). The flux at the focal point can be controlled in a range of 1 to 250 W/cm^2 with the primary concentrator and 10 to 5000 W/cm^2 with the secondary concentrators.

Applications

Several types of surface-processing experiments are under investigation at the HFSF; these include surface hardening, cladding, diamond film-growth, superconductor film-growth, and ceramic metallization (Pitts et al., 1993). Other experiments include production of ceramic powders and fullerenes (Hale et al., 1994). Test samples used for surface processing are typically square, with sides ranging from 1 to 5 cm in length. The flux profile incident on the target must be somewhat uniform to promote uniform surface processing and prevent substrate failure due to thermally induced stresses. Disparities in incident flux lead to undesirable temperature gradients, which may result in fracturing of the substrate.

Flux Attenuation

We employ two different attenuators at the HFSF to control the amount of sunlight reaching the target. A sliding-plate attenuator is used primarily when the facets are aimed at the same target point to produce the maximum amount of concentration possible. This attenuator consists of two plates which move vertically in opposite directions, creating an aperture between the primary concentrator and the focal point (Figure 1). This arrangement works well on smaller samples of less than 2 cm on a side. On larger targets, however, this focusing strategy causes inequities in the flux distribution due to the Gaussian nature of the beam; that is, the center of the targets are exposed to higher levels of concentration than are the edges.

The sliding-plate attenuator is located 5.2 meters from the center of the primary concentrator array and 1.8 meters in front of the focal point. At this location, the image from each concentrator facet is still discrete. At high attenuation levels (i.e., when the attenuator is only opened a small amount), sunlight from only a

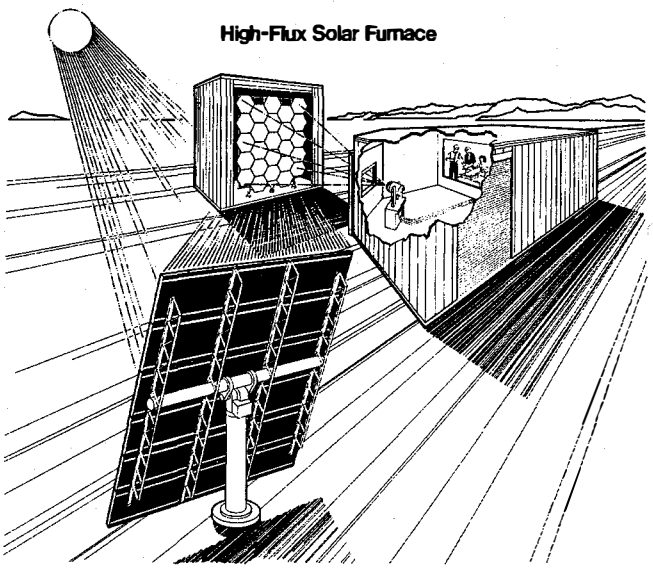

FIGURE 1. SCHEMATIC OF THE HFSF, SHOWING THE HELIOSTAT, FACETED PRIMARY CONCENTRATOR, AND SLIDING-PLATE ATTENUATOR ON THE EXTERIOR OF THE EXPERIMENT BUILDING

few facets falls on the target. Given that each facet has a separate aim point, this causes significant flux distribution inequities on the target.

The alternate attenuator resembles a venetian blind and is similar to the attenuation systems employed at other solar furnaces. Sunlight from each of the facets is attenuated. Unlike the systems at other facilities, however, the device at the HFSF is positioned between the concentrator and the focal point, not between the heliostat and the primary concentrator. Such a location for the attenuator is possible at the HFSF due to its long focal-length-to-diameter ratio.

The venetian-blind attenuating system, shown in Figure 2, is small enough and light enough that it can easily be carried and installed by two people. The venetian-blind attenuator is installed directly in front of the sliding-plate attenuator, which is an integral piece of the HFSF. When the venetian-blind attenuator is in place, the sliding-plate attenuator is opened to its fullest extent. Both attenuator systems are driven by stepper motors and can be controlled in either manual or automatic modes. At the location of the attenuators, peak concentrations are on the order of 25 suns; thus, active cooling is not required.

Each attenuation system has its advantages and disadvantages. The sliding-plate attenuator provides good control when the primary facets are aimed for peak concentrations and does not block any sunlight when in the fully-open position. It does not provide uniform illumination of the target at high attenuation levels when the primary facets are aimed for a broader flux pattern at the focal point. In contrast, the venetian-blind attenuator does provide good control at high attenuation levels when the primary facets are re-aimed for a broader flux pattern. However, it blocks a certain amount of sunlight in its full-open position.

PROCEDURE

To investigate and demonstrate the performance of the two systems, we performed the following tests.

Instrumentation

Flux distributions at the focal point of the HFSF are measured with a video-camera-based flux-mapping system. A charge-coupled-device video camera captures reflected sunlight from a diffusely reflecting, water-cooled plate located at the focal point. Circular foil calorimeters located on one side of the water-cooled plate are used to quantify peak concentrations. We use the BEAMCODE software system and the calorimeter readings to scale the captured video camera images, quantify the flux distributions, and calculate the total power available (Lewandowski et al., 1993).

We use a normal incidence pyrheliometer (NIP) to measure the direct-normal solar irradiance. The uncertainty of the circular foil calorimeters and the NIP data has been calculated to be ±3.6% and ±1.6%, respectively (Bingham, 1992).

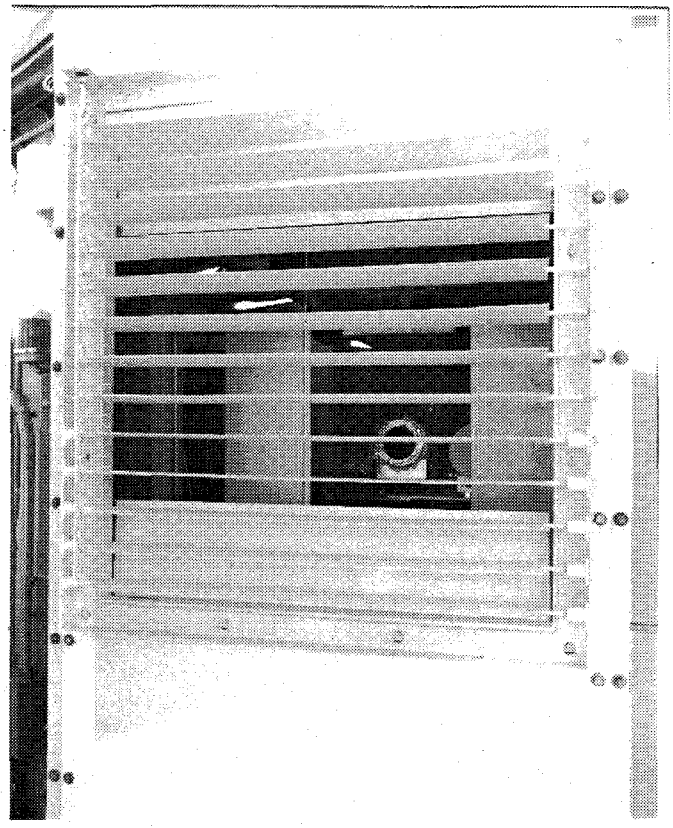

FIGURE 2. THE VENETIAN-BLIND ATTENUATOR, INSTALLED OVER THE SLIDING-PLATE ATTENUATOR WHERE THE BEAM ENTERS THE EXPERIMENT ROOM

Test Procedure

For each test, we used the 13 central facets of the primary concentrator. With the mirror facets aimed at a single point, the two attenuators were calibrated to provide power or peak flux as a function of attenuator position or opening. This allowed us to compare the flux distributions provided by the two attenuators at similar power levels.

With the primary facets aligned to a single point, flux maps and calorimeter readings were collected at several settings for both attenuators. We then aligned 13 of the primary facets to a hexagonal pattern at the target plane to produce a relatively uniform flux distribution over a 5-cm × 5-cm area at the focal point. Figure 3 shows the pattern used. This facet-aiming configuration was determined analytically using the SOLFUR ray-trace computer code (Jorgensen, 1991). Flux maps and calorimeter readings were taken at several settings with both attenuators and the re-aimed primary array.

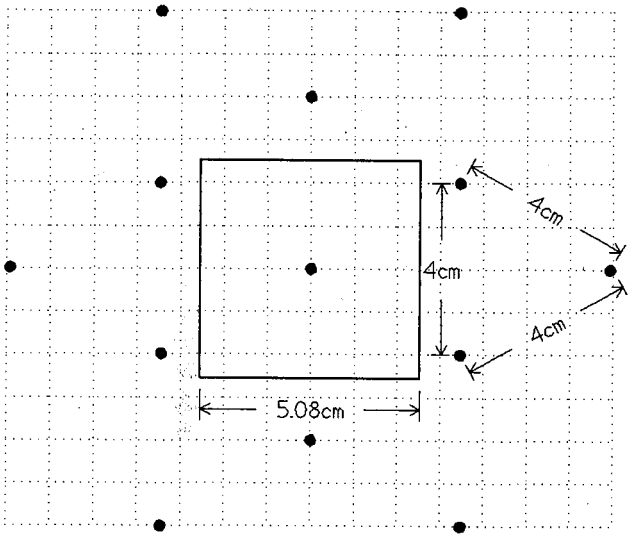

FIGURE 3. THE AIM PATTERN USED FOR TEST, USING 13 FACETS AIMED AT THESE POINTS 4 CM APART

RESULTS

Maximum concentration is possible with all the primary facets aimed at a single point. The measured peak intensity and the percentage of full power through a given aperture are two key relative values for this concentrator alignment. Peak concentrations using the sliding-plate attenuator were 1460 suns; peak concentrations using the venetian-blinds attenuator were 1400 suns. On average, the venetian blinds decrease the peak concentration by about 4% because the individual blinds block incoming sunlight even when fully open. Figure 4 is a graph of the percentage of full power in a 10-cm-diameter aperture located at the centroid of the image versus the total calculated power. All data were normalized to a NIP reading of 1000 W/m^2 to allow comparison of images and calorimeter data taken at varying levels of direct-normal irradiance.

Both attenuators provide a reasonably good regulation of the amount of power reaching the target. As mentioned, peak concentrations and higher power levels are possible with the sliding-plate attenuator. Also, given the lower overall percentage of full power through a 10-cm aperture, the venetian-blind attenuator appears to be scattering a significant amount of radiation, in addition to blocking or shading the target.

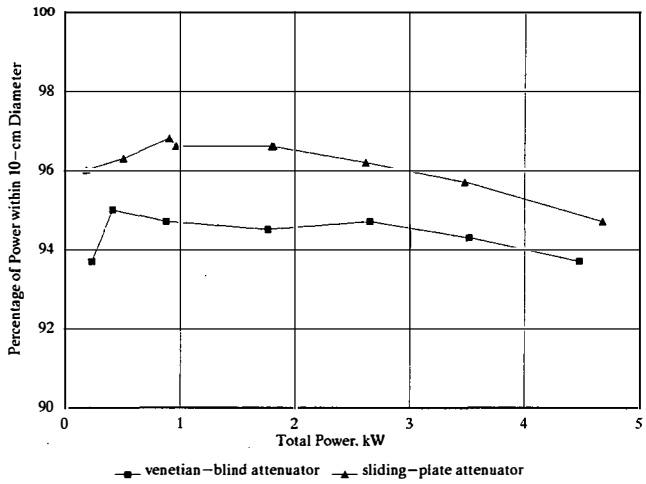

FIGURE 4. PLOT OF PERCENTAGE OF POWER WITHIN A 10-CM-DIAMETER APERTURE, FOR BOTH ATTENUATORS, AT ALL POWER LEVELS

The purpose of re-aiming the primary facets is to obtain minimal flux variation over a given area. Results from the two attenuators are shown in Figure 5, in which we plot the standard deviation of the intensity as a percentage of the mean intensity over a 5-cm × 5-cm area located at the centroid versus the calculated total power incident on the target. As shown previously in Figure 4, the venetian-blind attenuator blocks a noticeable fraction of the sunlight. Also evident in Figure 5 is the performance of the two systems at high attenuation levels. The venetian blinds provide a much more uniform flux distribution across the 5-cm × 5-cm sample area at low light levels. This result is also shown in Figures 6 and 7, which are surface plots of the intensity across the 5-cm × 5-cm samples centered about the centroid for the two systems, each positioned to provide about 5% of the peak flux.

The valleys in Figure 6 would normally be filled by sunlight reflected from a facet that was blocked by the sliding plate at this high attenuation level. At high attenuation levels, the aperture consists of a small horizontal slit that may be much smaller than the image of a single facet on the attenuator; for example, the slit may be 1 cm wide, whereas the width of the image of the full array of facets incident on the attenuator may be 1 m. Figure 7, the flux distribution for the venetian blinds, shows a much more even distribution.

CONCLUSIONS

The benefits of the two systems are evident from the above results. The sliding-plate attenuator works best by providing higher levels of power at higher peak concentrations when the primary facets are aimed to a single point. It will perform the best in tests that require the maximum absolute peak flux available. It

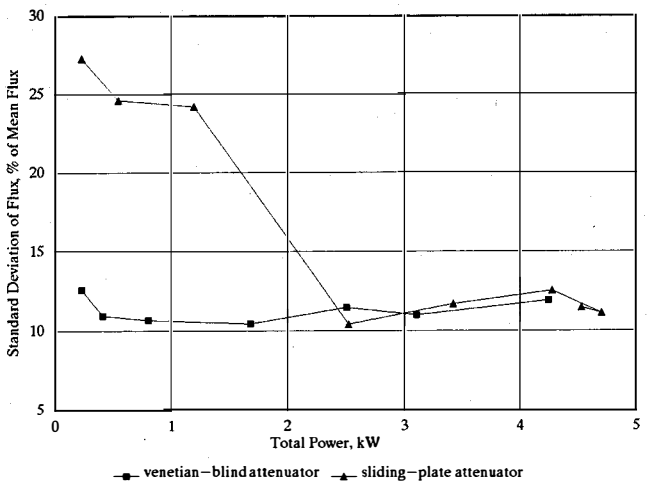

FIGURE 5. STANDARD DEVIATION OF INTENSITY AS A PERCENTAGE OF MEAN INTENSITY WITHIN A 5.08-CM SQUARE, FOR BOTH ATTENUATORS, AT ALL POWER LEVELS

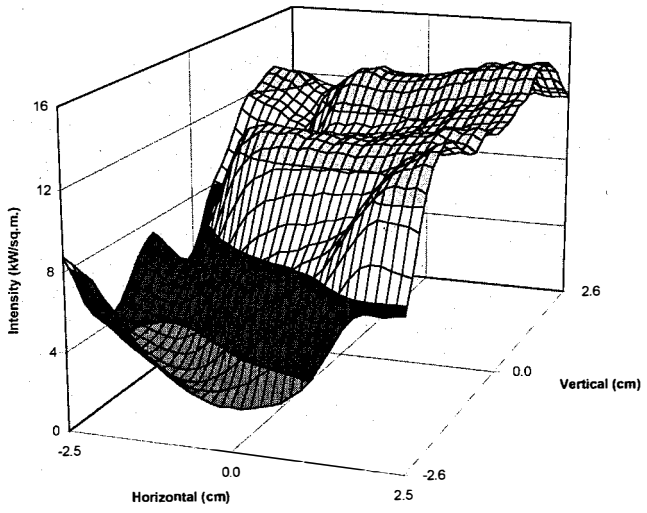

FIGURE 6. PLOT OF FLUX INTENSITY TO HORIZONTAL AND VERTICAL DIMENSIONS IN A 5.08-CM SQUARE AT 5% POWER, USING THE SLIDING-PLATE ATTENUATOR

also provides higher overall concentrations at low levels of attenuation when the facets are re-aimed to provide uniform intensity at the target plane. The venetian-blind attenuator is far superior at providing uniform illumination at high levels of attenuation with a distributed concentrator aiming configuration. It can also be used in tests that don't require large peak concentrations, i.e., over 2000 suns.

Many surface-processing tests require a slow increase in intensity to properly process the materials and minimize thermal stresses on the substrate. The venetian-blind attenuator allows the processing of the samples with a consistently uniform flux distribution at all power levels.

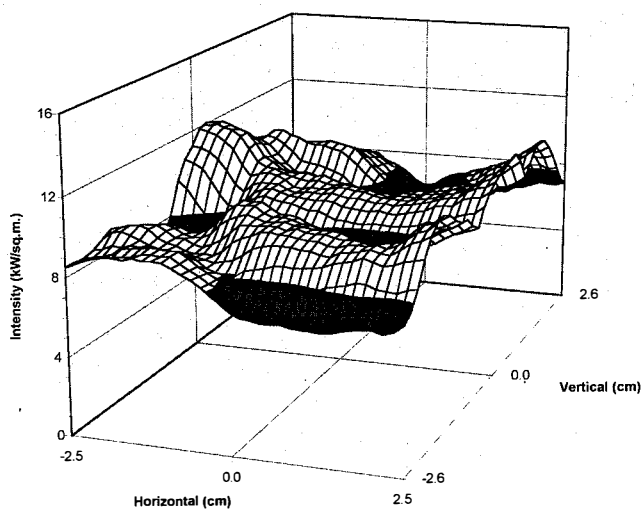

FIGURE 7. PLOT OF FLUX INTENSITY TO HORIZONTAL AND VERTICAL DIMENSIONS IN A 5.08-CM SQUARE AT 5% POWER, USING VENETIAN-BLIND ATTENUATOR

ACKNOWLEDGMENTS

The authors wish to acknowledge Judy Netter, who assisted in the operation of the furnace and collection of data for this paper, and George Yeagle, who fabricated the flux-mapping plate and the venetian-blind attenuator.

REFERENCES

Bingham, C., 1992, "Uncertainty of Calorimeter Measurements at NREL's High Flux Solar Furnace," *Proceedings of the 1992 ASME/JSME/JSES International Solar Energy Conference*, Maui, HI, April 4–8, 1992, pp. 1231–1237.

Bingham, C., and Lewandowski, A., 1991, "Capabilities of SERI's High Flux Solar Furnace," *Proceedings of the 1991 ASME/JSME/JSES International Solar Energy Conference*, Reno, NV, March 17–22, 1991, pp. 541–545.

Hale, M.J., Fields, C., Lewandowski, A., Bingham, C., and Pitts, J., 1994, "Production of Fullerenes with Concentrated Solar Flux," *Proceedings of the 1994 ASME/JSME/JSES International Solar Energy Conference*, San Francisco, CA, March 27–30, 1994, pp. 93–101.

Jenkins, D., Winston, R., O'Gallagher, J., Lando, M., Bernstein, H., and Lewandowski, A., 1994, "Applications of Ultra-High Solar Flux," *Solar 94: Proceedings of the 1994 Annual Conference, American Solar Energy Society*, San Jose, CA, June 27–30, 1994, pp. 413–417.

Jorgensen, G., 1991, "Comparison of Predicted Optical Performance with Measured Results for Dish Concentrators," *Proceedings of the Biennial Congress of the International Solar Energy Society,* Denver, CO, August 19–23, 1991, Vol. 2, Part 1, pp. 2031–2036.

Lewandowski, C., Scholl, K., and Bingham, C., 1993, "Modification of Flux Profiles Using a Faceted Concentrator," *Solar 93: Proceedings of the 1993 Annual Conference, American Solar Energy Society*, Washington, D.C., April 25–28, 1993,

pp.229–234.

Pitts, J.R., Tracy, E., Shinton, Y., and Fields, C., 1993, "Applications of Solar Energy to Surface Modification Processes," *Critical Reviews in Surface Chemistry*, Vol. 2, No. 4, pp. 247-269.